

Bacterial respiratory chain diversity reveals a cytochrome c oxidase reducing O₂ at low overpotentials

Xie Wang,[†] Romain Clément,[†] Magali Roger,[‡] Marielle Bauzan,[§] Ievgen Mazurenko,[†] Anne de Poulpiquet,[†] Marianne Ilbert,[†] Elisabeth Lojou^{*†}.

^[a] Aix-Marseille Univ, CNRS, BIP, UMR 7281, 31 Chemin Aiguier, 13009 Marseille, France.

^[b] School of Natural and Environmental Sciences; Newcastle University, Devonshire building, NE1 7RX, Newcastle upon Tyne, England.

^[c] Aix-Marseille Univ, CNRS, IMM, FR 3479, 31 Chemin Aiguier, 13009 Marseille, France.

Supporting Information

Contents

S1. General methods

S1.1 Chemicals and materials

S1.2 Purification of *A. ferrooxidans* Cyt *c*₄

S2. Determination of redox midpoint potentials by redox titration

S3 Determination of the second order rate constants

S3.1 Diffusing redox mediators

S3.2 Redox mediators in thin layer

Supplementary figures

Supplementary tables

References

S1 General methods

S1.1 Chemicals and materials

Absolute ethanol (EtOH), acetic acid (96%), 6-Aminocaproic acid (ACA), Ammonium Acetate (NH₄Ac), Ampicillin, Anti-protease (fast protease inhibitor tablets), DNase I from bovine pancreas, N,N-Dimethylformamide (DMF), DL-Dithiothreitol (DTT), Ethylenediaminetetraacetic acid disodium salt dehydrate (EDTA), Hydrochloric acid (HCl), Sulfuric acid (98% H₂SO₄), LB Broth (LB), N-Methyl-2-pyrrolidone (NMP), Sodium hydroxide, n-dodecyl β -d-maltoside (DDM), Potassium phosphate buffer (K₂HPO₄/KH₂PO₄), Sodium acetate (NaAc), Sodium chloride, Sodium dithionite (dithionite), Tris base (Tris), triton X100, urea, potassium ferricyanide (FeCN), ferrocenemethanol (FcMeOH) were bought from Sigma-Aldrich and used as received. Ferrocenecarboxylic acid (FC) was from Fluka.

CcO, aa₃ type from bovine heart and Cyt *c* from bovine heart were bought from Sigma Aldrich, and used with no further purification.

Bicinchoninic acid (BCA) was from Thermo Fisher Scientific, Diethylaminoethyl cellulose (Capto™ DEAE resin), and Cocomono-glyceride sulfonic acid resin (Mono S™ 5/50 GL column) were purchased by GE Healthcare. Bio-gel HTP hydroxyapatite was purchased from BIORAD.

All aqueous solutions were prepared with Milli Q (18.2 M Ω ·cm) water.

S1.2 Purification of *A. ferrooxidans* Cyt *c*₄

Cyt *c*₄ was expressed and purified from *E. coli* as recently described ¹. The protein concentration was determined by UV–Vis ABS spectroscopy, using the theoretical molar extinction coefficient (ϵ_{280}) of 23380 M⁻¹·cm⁻¹.

S2. Determination of redox midpoint potentials by redox titration

Optical redox titrations were carried out at 25 °C as described by Dutton ³, using a Kontron Uvikon 922 double-beam spectrophotometer equipped with a Spectralon integrating sphere. Membrane fragments were suspended in 50 mM potassium phosphate buffer (pH 7.4); pH values were controlled at the beginning and at the end of each redox titration. The following redox mediators were used at 10 μ M concentrations: 1,1'-ferrocenedicarboxylic acid, ferrocenemonocarboxylic acid, 1,4-benzoquinone, *N,N,N',N'*-tetramethyl-*p*-

phenylenediamine, 2,5-dimethyl-*p*-benzoquinone, 1,2-naphthoquinone, 1,4-naphthoquinone, phenazine ethosulfate, indigo carmine, anthraquinone-2,6-disulfonate, and anthraquinone-2-sulfonate. Reductive titrations were carried out using sodium dithionite, and oxidative titrations were done using sodium hexachloroiridate (Na₂Cl₆Ir).

S3 Determination of the second order rate constants

S3.1 Diffusing redox mediators

The rate of the reaction between CcO and the artificial redox mediators (FeCN, FcMeOH, and FC) was calculating according to the theory of Nicholson and Shain ⁴. In those cases, in the absence of O₂, diffusion of the redox mediators are attested by the linear increase of the peak currents, *I*_p, with the square root of the scan rate *v*. The ratio of the limiting catalytic current, *i*_{cat}, obtained under O₂ and the diffusion-controlled peak current *i*_p versus the reciprocal scan rate *v* allows the determination of the pseudo first order rate constant, *k'*, according to :

$$(i_{cat}/i_p)^2 = \lambda = k'(RT/nF)v$$

Given the CcO concentration, the second order rate constant *k* can be calculated.

S3.2 Redox mediators in thin layer

When the redox mediators (Cyt *c*₄ or Cyt *c*) are entrapped in the thin layer at the PG membrane electrode, the second order rate constants, *k*, between cytochromes and CcO were modeled by COMSOL software.

The graphite electrode is a macro-electrode (3 mm diameter), so we can make the assumption that the transport across its surface is uniform. Therefore, only physics occurring normal to the surface has to be considered and 1D model is sufficient. The model contains a single 1D domain of length *L*, where *L* is the maximum size of the diffusion layer over the duration of the electrochemical experiment.

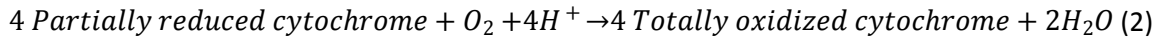
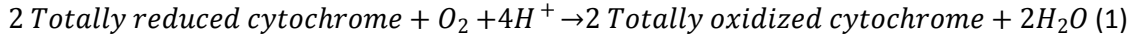
To model the dialysis membrane used to confine the proteins in the vicinity of the electrode, we introduce a thin diffusion barrier permeable to O₂ but impermeable to the proteins. The diffusion coefficients through the membrane are set respectively to *D*_{O2}=*D*_{O2, bulk} and *D*_{Protein}=0.

The electroanalysis interface assumes that a large quantity of supporting electrolyte makes the resistance low enough to neglect the electric field in the solution: $\Phi_i=0$.

The chemical transport of electroactive species over the domain obeys second Fick's law:

$$\frac{\partial c_i}{\partial t} = \nabla \cdot (D_i \nabla c_i) + R_i$$

Where R_i are the rates of the chemical reactions occurring in the electrolyte. The enzyme-catalyzed reactions between dioxygen and the cytochromes occur in the thin layer between the electrode and the dialysis membrane.



H_2O and H^+ are not considered since we consider they do not affect the electrochemical response. We consider the rates of the reactions (1) and (2) obey Michaelis-Menten kinetics with respect to oxygen and first order kinetics with respect to cytochrome so that the reaction rates are given by:

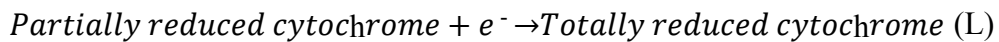
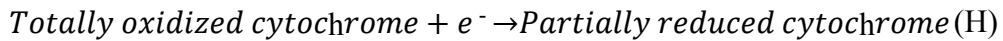
$$R_1 = k_{cat,1} \frac{c_{O_2}}{K_m + c_{O_2}} c_L$$

$$R_2 = k_{cat,2} \frac{c_{O_2}}{K_m + c_{O_2}} c_H$$

where c_L and c_H are respectively the concentrations of totally and partially reduced cytochrome.

Boundary conditions:

At the bulk boundary ($x=L$), O_2 concentration equals the O_2 saturation concentration at the given temperature. At the electrode boundary ($x=0$), we consider two successive one-electron transfer. The totally oxidized cytochrome reduces to give the partially reduced cytochrome that in turns reduces to give the totally reduced cytochrome. Electron is transferred either from $Heme_H$ (reaction H) or from $Heme_L$ (reaction L):



The current density for each reaction is given by the electroanalytical Butler-Volmer equation:

$$i_{loc} = nFk_0 \left(c_{Red} \exp \left(\frac{(n - \alpha_c)F\eta}{RT} \right) - c_{Ox} \exp \left(\frac{-\alpha_c F\eta}{RT} \right) \right)$$

where k_0 is the heterogeneous electron transfer rate constant and α_c the cathodic transfer coefficient (set to 0.5).

The flux is proportional to the current density, according to Faraday's law:

$$-n.N_i = \frac{v_i i_{loc}}{nF}$$

And the total electrode current is obtained by multiplying the local current density by the electrode surface:

$$I_{electrode} = i_{loc}A$$

The potential applied at the electrode follows a triangular waveform consistently with a cyclic voltammetry experiment. The potential is scanned accordingly between $E_{vertex1} = 0.6$ V vs. NHE and $E_{vertex2} = 0.175$ V vs. NHE at a constant scan rate v . The equilibrium potentials of heme L and heme H are set respectively to $E_H = 0.43$ V vs. NHE and $E_L = 0.31$ V vs. NHE (experimentally found values at pH 4.8).

Successive parametric sweeps are conducted to consider the influence of different parameters. First the non-catalytic curves of the model are fitted to the experimental curves (cytochrome and CcO in the absence of O_2) to fix the length of the diffusion layer limited by the dialysis membrane (position of the semi permeable barrier) and determine the dilution factor induced by the membrane configuration. To obtain the catalytic rate constants the required parameters are set to the values indicated below:

Parameter	Value[Unit]
Voltammetric scan rate	5.10^{-3} [V/s]
Introduced Cyt c_4 concentration c_{cyt}	50.10^{-6} [mol/L]
Dilution factor d_f (dimensionless)	4.6
Initial concentration of totally oxidized Cyt c_4 at electrode $c_{initial1}$	c_{cyt}/d_f [mol/L]
Initial concentration of partially reduced Cyt c_4 at electrode $c_{initial2}$	$c_{initial1}/(1+\exp((E_{vertex1}-E_{10})*F/(R*T)))$ [mol/L]
Initial concentration of totally reduced Cyt c_4 at electrode	$c_{initial2}/(1+\exp((E_{vertex1}-E_{20})*F/(R*T)))$ [mol/L]
Oxygen saturation concentration at 298 K	258.10^{-6} [mol/L]
Totally reduced Cyt c_4 diffusion coefficient D	1.10^{-10} [m ² /s]
Partially reduced Cyt c_4 diffusion coefficient D	1.10^{-10} [m ² /s]
Totally oxidized Cyt c_4 diffusion coefficient D	1.10^{-10} [m ² /s]

O₂ diffusion coefficient	0.8.10 ⁻⁸ [m ² /s]
First electrode reaction rate K01 (dimensionless)	1.10 ⁸
Second electrode reaction rate K02 (dimensionless)	3000
Electrode radius r_e	0.0015 [m]
First electrode reaction rate	K01*D/r _e [/s]
Second electrode reaction rate	K02*D/r _e [/s]
Double layer capacitance	0.15 [F/ m ²]
Temperature	298.15 [K]
Start potential	0.6 [V vs. NHE]
Switching potential	0.175 [V vs. NHE]
First Equilibrium potential	0.43 [V vs. NHE]
Second Equilibrium potential	0.31 [V vs. NHE]
cytochrome-O₂ Michaelis Menten constant	1.10 ⁻⁶ [mol/L]
Outer bound on diffusion layer	6*sqrt(D*2*abs(E_vertex1-E_vertex2)/v) [m]
Position of the semi permeable barrier	22.10 ⁻⁶ [m]

The second order rate constants k were obtained by dividing k_{cat} values deduced from the modeling by the CcO concentration under the dialysis membrane.

Supplementary figures

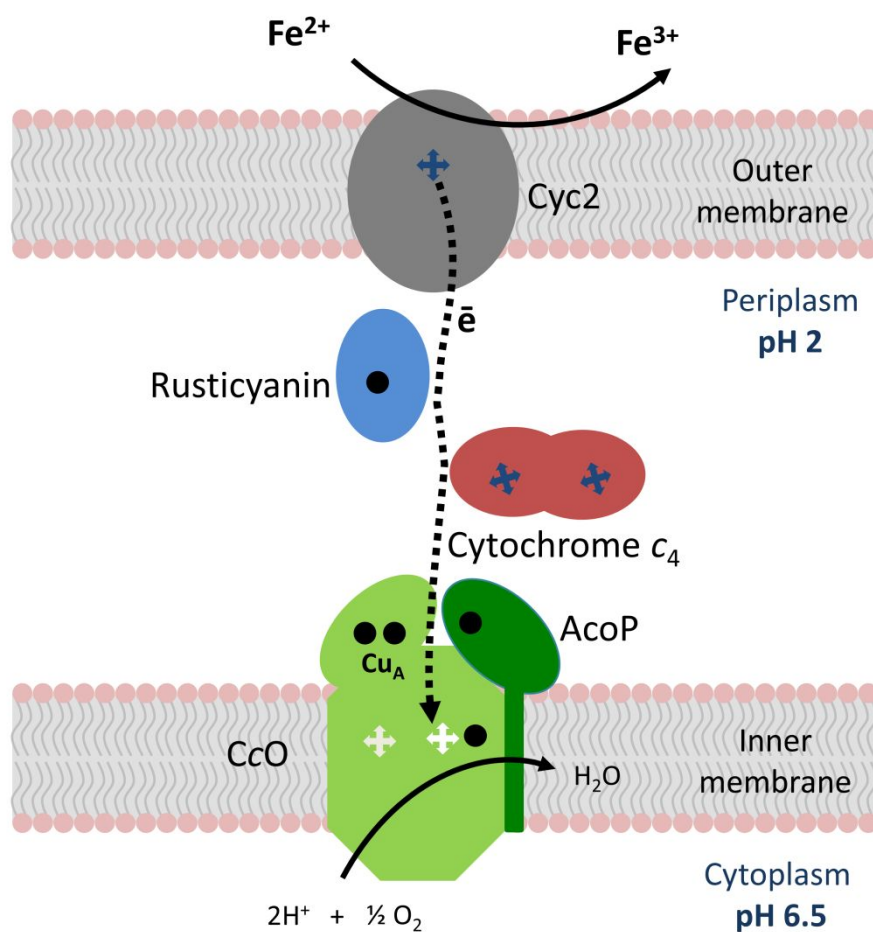


Figure S1: Ferrous iron oxidation pathway of *Acidithiobacillus ferrooxidans*. *A. ferrooxidans* can oxidize Fe^{2+} into Fe^{3+} using a chain of metalloproteins that span the outer membrane (via the cytochrome Cyc2) to the inner membrane via the soluble periplasm (through the copper protein, Rusticyanin in blue and the dihemic cytochrome c_4 in red). Electrons generated allows the reduction of O_2 into water via the integral inner-membrane CcO (light green). AcoP (dark green) is a copper binding protein with a transmembrane segment, this protein copurifies with CcO. Heme centers are depicted with white crosses, and copper centers are depicted with black circles.

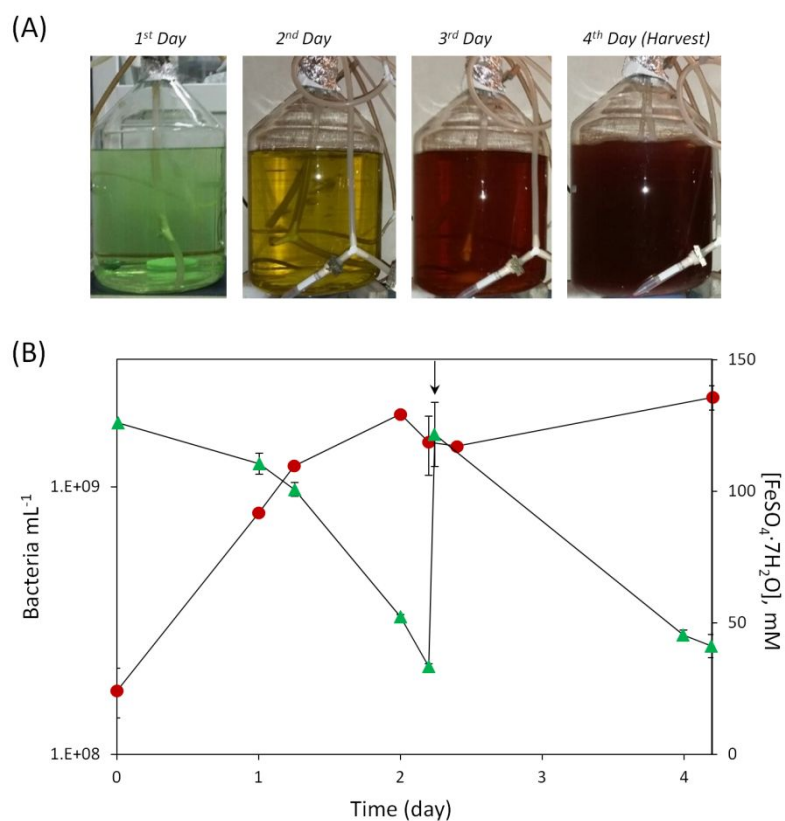


Figure S2 The yield of biomass was improved by addition of ferrous iron during the bacteria growth. (A) Photographs showing the growth of bacterial biomass along with accumulation of oxidized forms of iron; 20 L of culture are shown on different day of growth; (B): Growth curve of *A. ferrooxidans* in semi-logarithmic plot (red curve), and ferrous iron concentration (green curve). Addition of supplemental ferrous iron is indicated by the arrow.

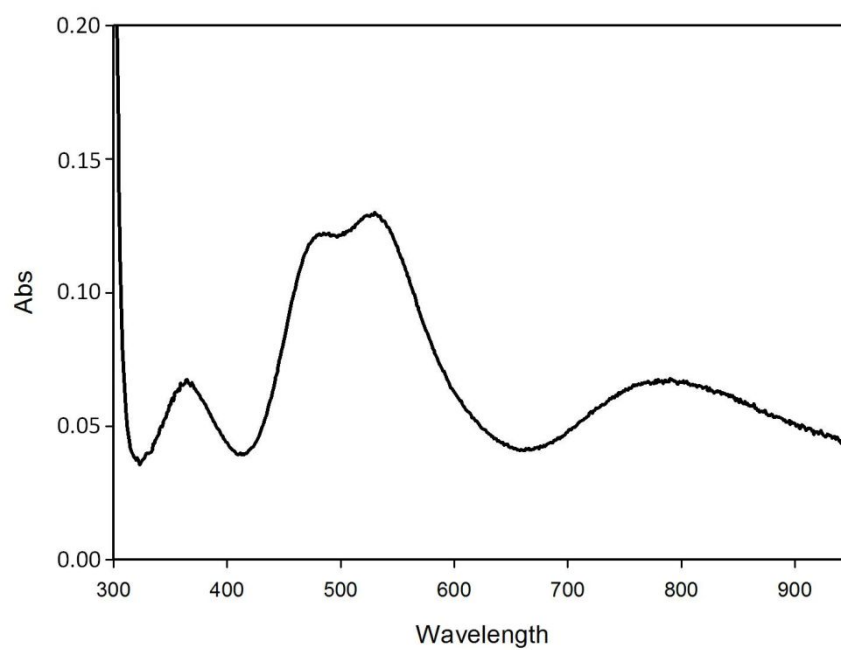


Figure S3 UV-visible spectrum of 50 μ M CoxB 50 mM NaAc pH 5, showing the typical bands assigned to the Cu_A .

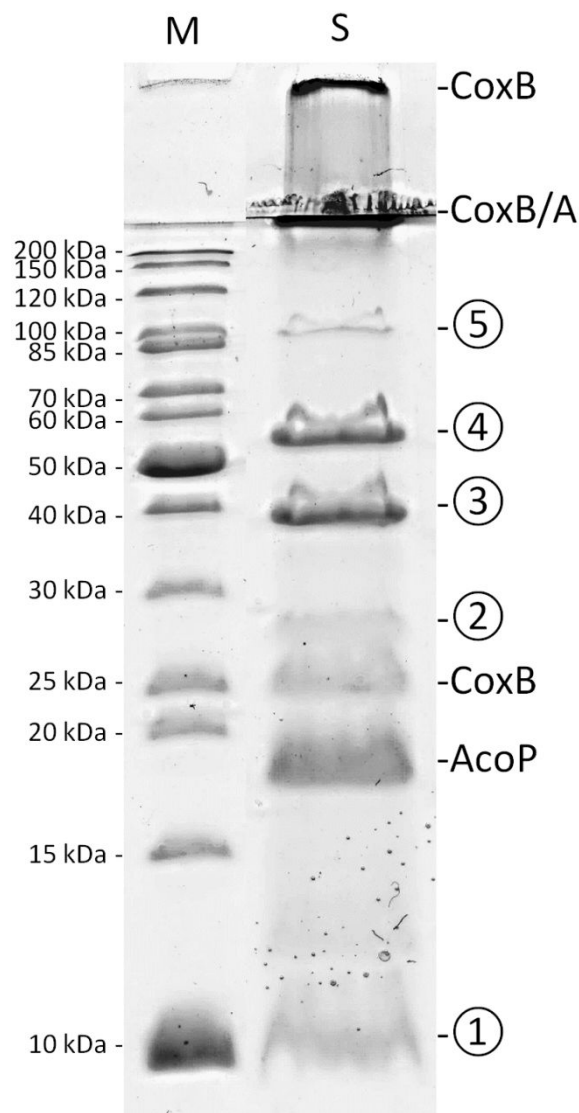


Figure S4 *A. ferrooxidans* AcoP copurifies with CcO. M: protein ladder, with the size of standard proteins shown on the left of the gel. S: 34 μ g of protein sample. Each band was identified by liquid chromatography–mass spectrometry after enzymatic digestion. Bands corresponding to CcO, i.e. AcoP, and the two main sub-units CoxB (Cu_A domain) and CoxA are indicated on the gel. Bands ① - ⑤ correspond to lipoprotein, OmpA, Omp40, Cyc2 and TonB, respectively.

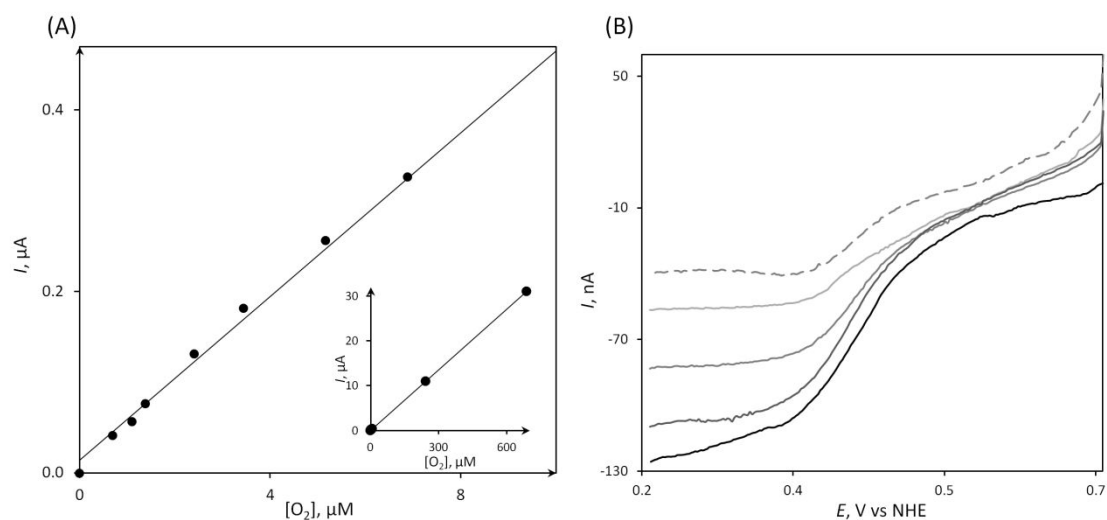


Figure S5 (A) O_2 concentration calibration curve. The calibration curve was obtained by relating oxygen reduction current to oxygen concentration at a platinum electrode. A larger scale is shown in the insert. (B) CVs of $14\ \mu\text{M}$ CcO in the presence of $40\ \mu\text{M}$ FcMeOH and increasing concentrations of O_2 : $0\ \mu\text{M}$ (dotted line), $0.69\ \mu\text{M}$, $5.12\ \mu\text{M}$, $13.48\ \mu\text{M}$ and $26.44\ \mu\text{M}$. The catalytic current was measured at $+350\ \text{mV}$ after subtraction of the current for the mediator alone. All the experiments are carried out in an anaerobic glove box.

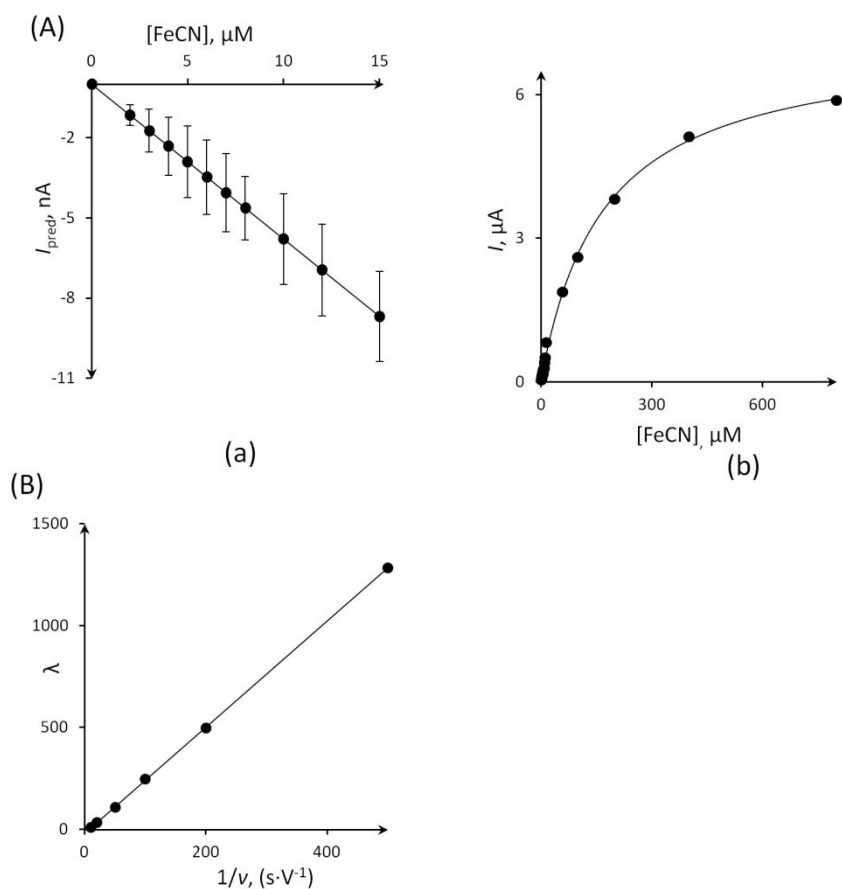


Figure S6 Determination of the kinetic constants between FeCN and CcO of *A. ferrooxidans*. Panel (A) : K_M Determination for FeCN: (a) Linear relationship between FeCN concentration and the cathodic peak current, (b) Relationship between the mediated catalytic current and FeCN concentration under O_2 fitted to Michaelis Menten equation. $14 \mu\text{M}$ CcO of *A. ferrooxidans* was entrapped at the PG membrane electrode; Panel (B): Determination of the second order rate constant between CcO and FeCN: plot of the kinetic parameter, λ , as a function of $1/v$ as detailed in S3. $14 \mu\text{M}$ CcO of *A. ferrooxidans* was entrapped at the PG membrane electrode in the presence of $20 \mu\text{M}$ FeCN in solution. 20 mM NH_4Ac buffer, pH 4.8. Scan rate $5 \text{ mV} \cdot \text{s}^{-1}$.

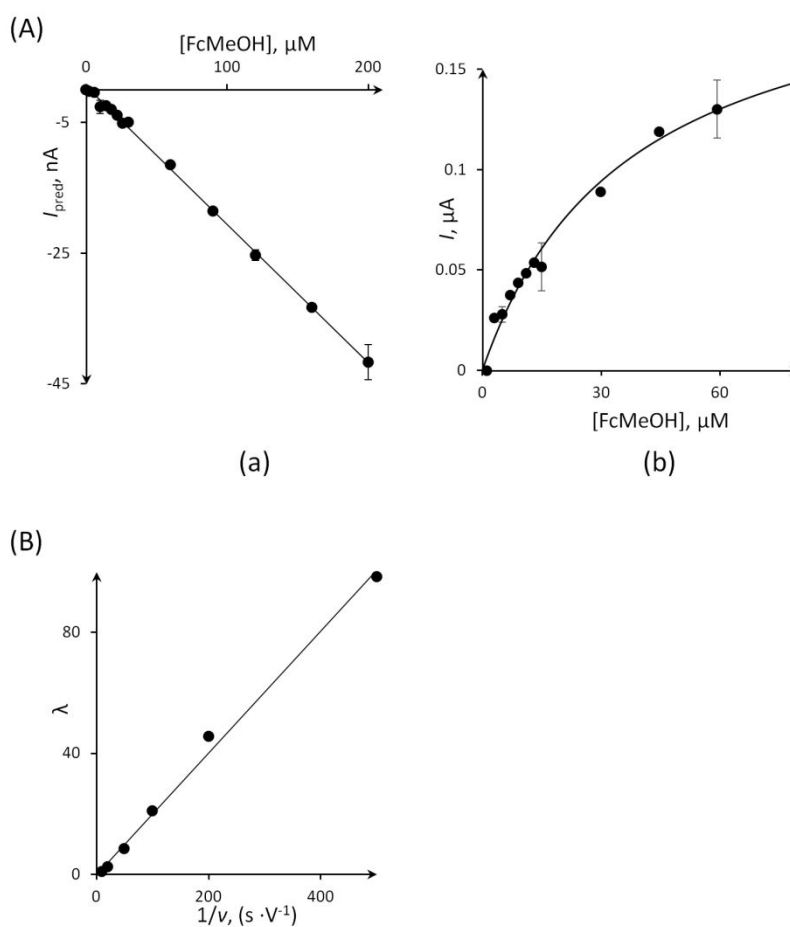


Figure S7 Determination of the kinetic constants between FcMeOH and CcO of *A. ferrooxidans*. Panel (A): K_M Determination for FcMeOH: (a) Linear relationship between FcMeOH concentration and the cathodic peak current, (b) Relationship between the mediated catalytic current and FcMeOH concentration under O_2 fitted to Michaelis Menten equation. 19 μM CcO of *A. ferrooxidans* was entrapped at the PG membrane electrode; 20 mM NH_4Ac buffer, pH 4.8. 5 $\text{mV} \cdot \text{s}^{-1}$. Panel (B): Determination of the second order rate constant between CcO and FcMeOH: plot of the kinetic parameter, λ , as a function of $1/v$ as detailed in S3. 19 μM CcO of *A. ferrooxidans* was entrapped at the PG membrane electrode in the presence of 5 μM FcMeOH in solution. 20 mM NH_4Ac buffer, pH 4.8.

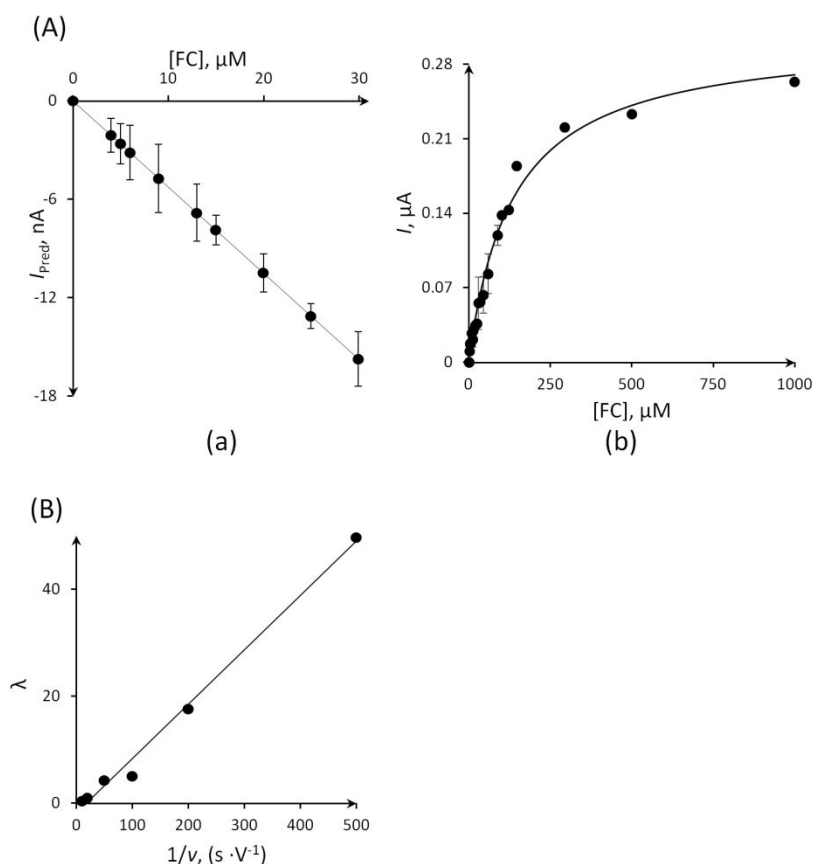


Figure S8 Determination of the kinetic constants between FC and CcO of *A. ferrooxidans*. Panel (A) : K_M Determination for FC: (a) Linear relationship between FC concentration and the cathodic peak current, (b) Relationship between the mediated catalytic current and FC concentration under O_2 fitted to Michaelis Menten equation. 14 μM CcO of *A. ferrooxidans* was entrapped at the PG membrane electrode; 20 mM NH_4Ac buffer, pH 4.8. 5 $mV \cdot s^{-1}$. Panel (B): Determination of the second order rate constant between CcO and FC: (b) plot of the kinetic parameter, λ , as a function of $1/v$ as detailed in S3. 14 μM CcO of *A. ferrooxidans* was entrapped at the PG membrane electrode in the presence of 13 μM FC in solution. 20 mM NH_4Ac buffer, pH 4.8.

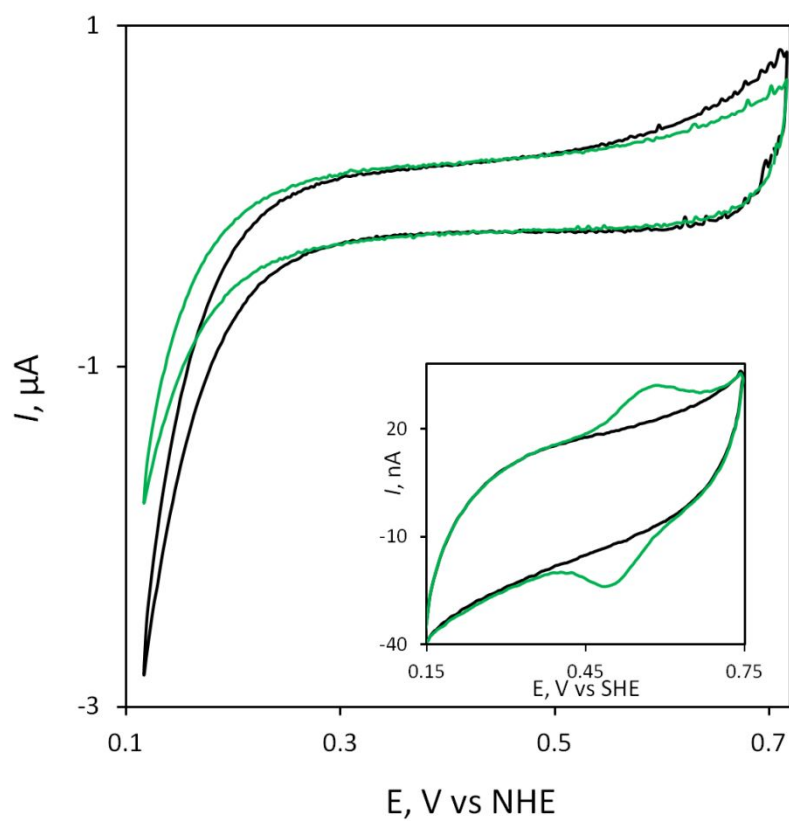


Figure S9 AcoP electrochemical behavior on CNF. CVs under O_2 atmosphere on CNF modified PG electrode before (black line) and after $14 \mu M$ AcoP adsorption (Green line). Insert: Positive control of the same AcoP sample at the PG membrane electrode. NH_4Ac 20 mM pH 4.8. Scan rate: 5 mV s^{-1}

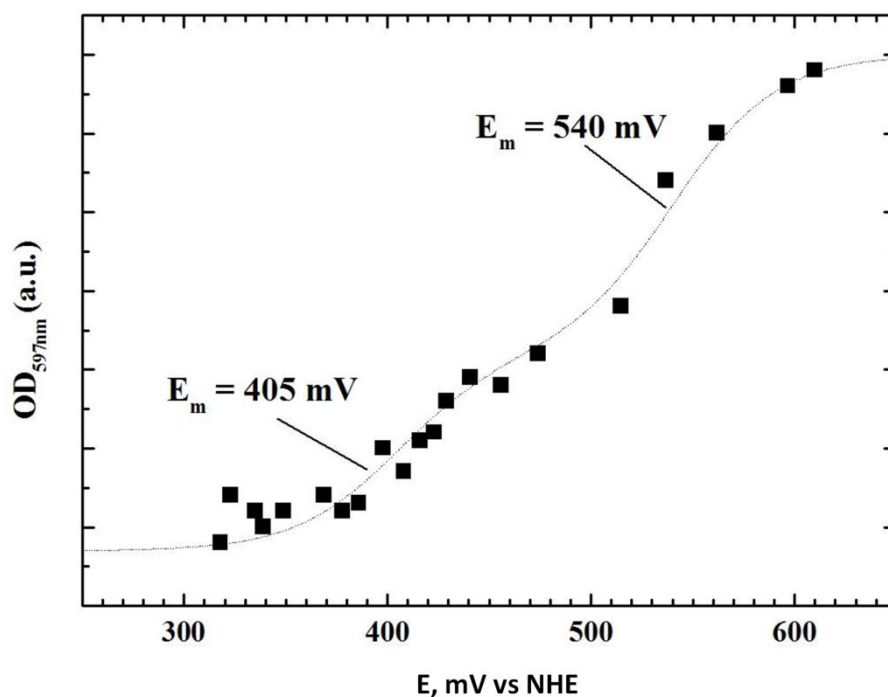


Figure S10 Determination of *A. ferrooxidans* CcO redox potential obtained by amperometric titration. Redox titration of CcO at pH 7.4 in 50 mM potassium phosphate buffer. Dependence of signal amplitude of the 597 nm peak arising from hemes *a* and *a*₃ on ambient redox potential, determined on membrane fragments from *A. ferrooxidans*. The obtained data points were fitted to two independent $n = 1$ Nernst curves yielding the indicated E_m values for the two titration waves.

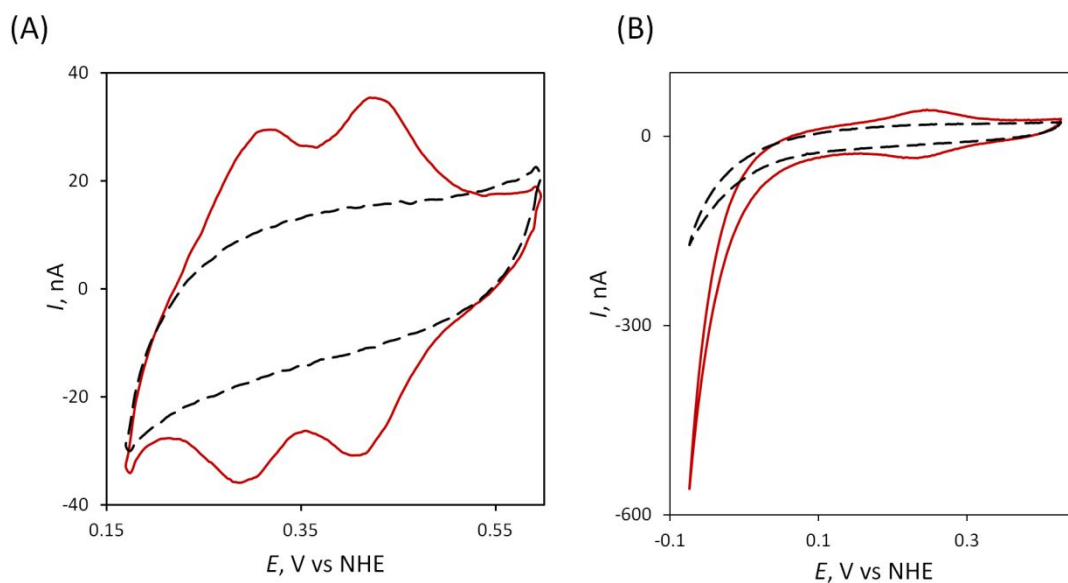


Figure S11 CVs of *A. ferrooxidans* Cyt *c*₄ and bovine heart Cyt *c* under O₂ atmosphere at PG electrode in the membrane configuration. (A) CVs before (black dashed line) and after 50 μM Cyt *c*₄ addition (red line) at the membrane PG electrode. NH₄Ac 20 mM, pH 4.8; (B) CVs before (black line) and after 50 μM bovine heart Cyt *c* addition (red line) at the membrane PG electrode. Phosphate buffer 20 mM, pH 7. Scan rate: 5 mV s⁻¹

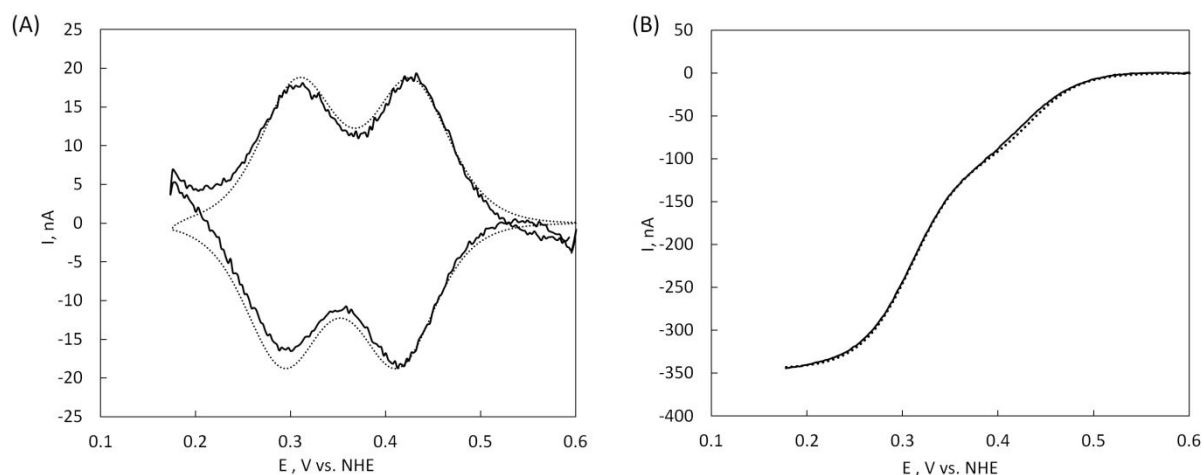


Figure S12 Determination of the second order rate constants between *A. ferrooxidans* CcO and Heme_L and Heme_H of Cyt c_4 : (A) Determination of the diffusion length and Cyt c_4 concentration: experimental CV of Cyt c_4 (solid line) and COMSOL model (dashed line); (B) Determination of the catalytic rate constants of the first and second O₂ reduction waves: experimental CV of O₂ reduction by CcO mediated by Cyt c_4 (solid line) and COMSOL model (dashed line). 2.5 μ M CcO of *A. ferrooxidans* was incubated with 50 μ M Cyt c_4 and entrapped at the PG membrane electrode 20 mM NH₄Ac buffer, pH 4.8. Scan rate: 5 mV s⁻¹.

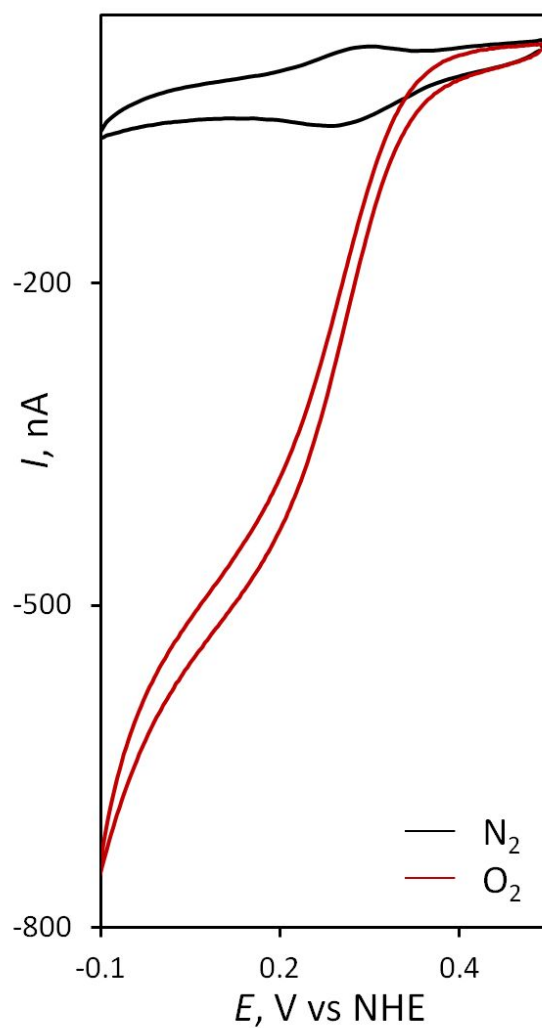


Figure S13 O_2 reduction by bovine CcO mediated by bovine heart Cyt c at the PG membrane electrode. 50 μ M Cyt c in the absence of CcO (Black curve), 50 μ M Cyt c in the presence of 4 μ M CcO (Red curve). 20 mM KH_2PO_4/K_2HPO_4 buffer, pH 7. Scan rate: 5 mV s^{-1} .

Supplementary tables

	E , V vs NHE at pH7	$K_{M(app)}$, μM	k , $10^5 \text{ M}^{-1} \cdot \text{s}^{-1}$
$\text{Ru}(\text{NH}_3)_6\text{Cl}_3$	-0.19	ND	ND
Cyt <i>c</i> Bovine	0.23	ND	4.1
$[\text{Fe}(\text{CN})_6]^{3-}$	0.37	-	-

Table S1 Kinetics data for bovine CcO obtained at the PG membrane electrode with either artificial redox mediators in solution or bovine heart Cyt *c* coimmobilized at the PG membrane electrode. ND means non determined data, and (-) means that no catalysis could be observed.

References

1. Wang, X.; Roger, M.; Clement, R.; Lecomte, S.; Biaso, F.; Abriata, L. A.; Mansuelle, P.; Mazurenko, I.; Giudici-Orticoni, M. T.; Lojou, E.; Ilbert, M., Electron transfer in an acidophilic bacterium: interaction between a diheme cytochrome and a cupredoxin. *Chem. Sci.* **2018**, *9*, 4879-4891.
2. Lappalainen, P.; Aasa, R.; Malmstrom, B. G.; Saraste, M., Soluble Cu(A)-binding domain from the *Paracoccus* cytochrome-c-oxidase. *J. Biol. Chem.* **1993**, *268*, 26416-26421.
3. Dutton, P. L., Oxidation-reduction potential dependence of interaction of cytochromes bacteriochlorophyll and carotenoids at 77 degrees K in chromatophores of chromatium-D and Rhodopseudomonas gelatinosa. *Biochim. Biophys. Acta* **1971**, *226*, 63.
4. Nicholson, R. S.; Shain, I., Theory of stationary electrode polarography for a chemical reaction coupled between 2 charge transfers. *Anal. Chem.* **1965**, *37*, 178.